Quasifission and fusion-fission lifetime studies for the superheavy element $Z = 120$

H. C. Manjunatha [1],[*] L. Seenappa,[1] P. S. Damodara Gupta,[2,3] N. Manjunatha,[1,2] K. N. Sridhar,[3] N. Sowmya,[1] and T. Nandi[4,*]

[1]*Department of Physics, Government College for Women, Kolar-563101, Karnataka, India*
[2]*Department of Physics, Rajah Serfoji Government College, Thiruchirappalli-620 024, India*
[3]*Department of Physics, Government First Grade College, Kolar-563101 Karnataka, India*
[4]*Inter University Accelerator Centre, Aruna Asaf Ali Marg, JNU New Campus, New Delhi 110067, India*

We study the quasifission and fusion-fission lifetimes for a number of fusion reactions used to synthesize the superheavy element $Z = 120$ using a statistical method within the framework of the dinuclear system model. In particular, influence of the target orientation and angular momentum on such lifetimes have been investigated. The quasifission and fusion-fission lifetimes have been compared very well with that of available experiments on successful superheavy element synthesis. We notice further the predicted quasifission and fusion-fission lifetimes of the projectile-target combinations used for the synthesis of the superheavy element $Z = 120$ also show the similar trend. Furthermore, the fusion-fission lifetime is seen to somewhat decrease with the increase of the angular momentum as well as beam energy. Little effect is seen on fusion barrier of the reaction and fission barrier of superheavy compound nucleus. Variation of quasifission lifetime is also not much with orientation angle, beam energy and fission barrier of the superheavy compound nuclei. Hence, this lifetime study does not provide any good reason why the attempted reactions have failed to synthesize the superheavy nuclei $Z = 120$. Furthermore, consideration of the fusion barrier, fissility, mass asymmetry, deformation parameter, fission barrier, etc., leads us to reveal that optimal colliding energy is important to have the largest evaporation residue cross section for any chosen reaction so that it is well within the measurable limit for a specific experimental set up.

I. INTRODUCTION

Great success has been achieved in the synthesis of the superheavy elements (SHE) formed in complete fusion reactions of heavy nuclei [1]. Both cold [2] and hot fusion reactions [3,4] have been used to produce the SHEs up to the element oganesson $Z = 118$ [5]. The cold fusion reactions have been used to synthesize superheavy elements up to $Z = 113$, whereas hot fusion reactions can produce superheavy elements up to $Z = 118$. These reactions are characterized by different entrance channels [6,7]. In cold fusion reactions, ^{208}Pb or ^{209}Bi target nuclei are bombarded with projectiles heavier than ^{48}Ca to form compound nuclei with low excitation energy of about 10 to 20 MeV. In hot fusion reactions ^{48}Ca projectile and actinide target nuclei are used with higher excitation energy between 30 and 60 MeV, which results in higher number of neutron evaporation [8] during formation of evaporation residues of the superheavy elements ($Z = 114$–118). To produce elements heavier than Oganesson $Z = 118$, projectiles heavier than ^{48}Ca has to be used, since the target elements heavier than californium ($Z = 98$) are not available [9,10]. The failed attempts in the synthesis of superheavy element 119 and 120 [1,11] indicate that the production cross sections are too small to be detected with the present detection system [12]. Hence, the latest interest of the synthesis of the superheavy element $Z > 118$ is in stake.

The superheavy elements are formed using the above said reactions in the laboratory by the fusion of two heavy nuclei [2–4]. According to the model of the formation of the dinuclear system [13–17], a large Coulomb repulsion forbids the sticking of the two heavy nuclei for a long while, rather it lasts for a short time and mostly the two nuclei usually come apart instead of undergoing a complete fusion, in a process called quasifission [16,18,19]. Finally, a smaller number of events that escaped from the quasifission and formed the compound nuclei, which either lose their excitation energy mainly by emission of particles and γ rays and goes to its ground state or undergo fission. Hence, the dominant reaction processes of the heavy ion-heavy target reactions are the quasifission and fusion-fission, which suppress strongly the formation of the evaporation residues. Synthesis of the superheavy elements $Z > 118$ requires an understanding of the reaction pathways leading to an evaporation residue, particularly quasifission and fusion-fission components. Quasifission occurs rapidly in a short interval of 10^{-20} s well before a compound nucleus is formed. In predicting the fusion reactions used to form the new superheavy elements it is very much necessary to understand the competition between the quasifission and fusion-fission [20]. Mass-angle distributions [21] provides the direct information on the characteristics and timescales of quasifission. A systematic study of carefully selected mass-angle distribution gives information on the quasifission, which is helpful in understanding of the shell effects, energy dissipation and the reaction pathways that suppress the formation of an evaporation residue [22]. The observed facts are in

---

*Corresponding author: manjunathhc@rediffmail.com; nanditapan@gmail.com

consonance with the predictions of the saddle point model [23].

Entrance channel effects such as target deformation and neutron richness determine the quasifission characteristics, which are the important issues in choosing a reaction for a new superheavy element [24]. Both the experimental and theoretical efforts have become vital to understand the fundamental as well as practical aspects of the quasifission [25]. The influence of shell effects on the formation of the fragments and the properties of quasifission fragments such as mass number, number of protons and neutrons, kinetic energy, and scattering angles have been studied systematically [26]. Kramers formula for the nuclear fission timescale is widely used as an extension to the width to account for large damping in the heavy-nuclei fission processes [27]. The yields of the quasifission products alone do not provide thorough information and hence the distribution of the total kinetic energy of the quasifission products is measured and calculated. The kinetic energy of the quasifission products depends on the deformations of the quasifission products [28]. The fragments of the quasifission with total kinetic energy follow the Viola systematics with long contact time of the order of 30 zs and large mass transfer similar to quasifission [29]. Signatures of quasifission have been studied for a range of reactions forming identical isotopes of curium. An evidence of the quasifission has been found in one or more detectable observable which will provide useful benchmark for future study [30]. The account of the shell effects in the deformation parameter of the colliding nuclei has a substantial influence on the characteristics of the combined system at the touching point as well as on the probability of the evaporation-residue formation [31]. The fusion cross sections are also calculated independently by using the extended-Wong model [32]. The dynamics of a system can be explained by using the appropriate Skyrme force whose parameters are fitted for the region to which it belongs [33]. The role of the angular momentum of the system in the emission of the complex fragments is studied and the reaction mechanism is determined by the angular momentum deposited in the system [34].

There has been conclusive evidence available for the quasifission and it is strongly dependent on the mean fissility. Quasifission occurs when the mean fissility value is less than 0.723 [35]. The calculated fusion-fission spectra do not show any asymmetric fission channels. It supports that the observed asymmetric channel emerging at the sub-barrier energy is the quasifission [36]. A modified Woods-Saxon potential model has been proposed for a unified description of the entrance channel fusion barrier and the fission barrier of the fusion-fission reactions based on the Skyrme energy-density functional approach [37]. The variation of total kinetic energy of the quasifission products is in agreement with the experimental data [19]. The fusion-fission events are much smaller than the quasifission events in the fusion reactions and thus, the quasifission process suppresses the complete fusion of the heavy nuclei [18] to a great extent.

Theoretical descriptions of nuclear viscosity are used [38] to understand the quasifission reaction dynamics. If the target is not deformed then it is found that the compound nucleus

formation is suppressed at sub-barrier energies and enhanced at above-barrier energies [39]. The quantitative studies of the angular momentum relaxation in quasifission reactions give information on both the time-dependent relaxation of the spin degrees of freedom and on the freeze-out geometry [40]. Timescales for the minimum and maximum possible mean excitation energies, the variation of the deduced fusion-fission timescale with the compound nucleus fissility has been studied [41]. The quasifission process is an important part of the total reaction cross section and gives the relation between the inelastic scattering processes and the complete fusion [42]. This fact is evident from the deviations from the predictions of the saddle point model because of not only complete fusion inside the fission barrier but rather a significant contribution from more direct reactions in which an approximate equilibration of the mass asymmetry and energy degrees of freedom is achieved. This reaction channel is referred to as the quasifission as defined above or sometimes the fast fission too and thus a fraction of the cross section originating from the complete fusion reaction only [43]. The fragment kinetic energy of the quasifission depends on the bombarding energy used for the projectile and target combination [44].

The quasifission and fusion-fission are known to be important hindrance in the formation of the compound nucleus. These phenomena can be studied using numbers of theoretical models, such as the Fokker-Planck equation, GRAZING model, CWKB model, DNS model, Langevin equations, time dependent Hartree-Fock model, and quantum molecular dynamics model as mentioned well by Wen *et al.* [45]. Out of these models the DNS model has become popular because of its simplicity and versatility. Besides the quasifission and fusion-fission, the DNS model describes the deep-inelastic collisions pretty well [45]. Even the dynamic nature of the nuclear reaction has been introduced very recently in this model [46]. The DNS model is still evolving in newer dimensions and any shortcoming of this model is yet to be known. By a natural choice at this stage, we have studied in the present work the competition between the quasifission and fusion-fission for all possible projectile target combinations used for the synthesis of the superheavy element 120 in terms of their lifetimes in the framework of the DNS model with the objective to find any clues behind the failing state of all the attempts till date.

II. THEORETICAL APPROACH

A. Quasifission lifetime

The quasifission lifetime of an asymmetric dinuclear system (DNS) in an excited state is given by [47,48]

$$\tau_{qf} = \frac{1}{\lambda_{qf}}, \qquad (1)$$

where λ_{qf} is the quasifission decay constant and is expressed as

$$\lambda_{qf} = \frac{\omega_m}{2\pi\omega_{qf}} \left(\sqrt{\left(\frac{\Gamma}{2\hbar}\right)^2 + \omega_{qf}^2} - \frac{\Gamma}{2\hbar} \right)$$
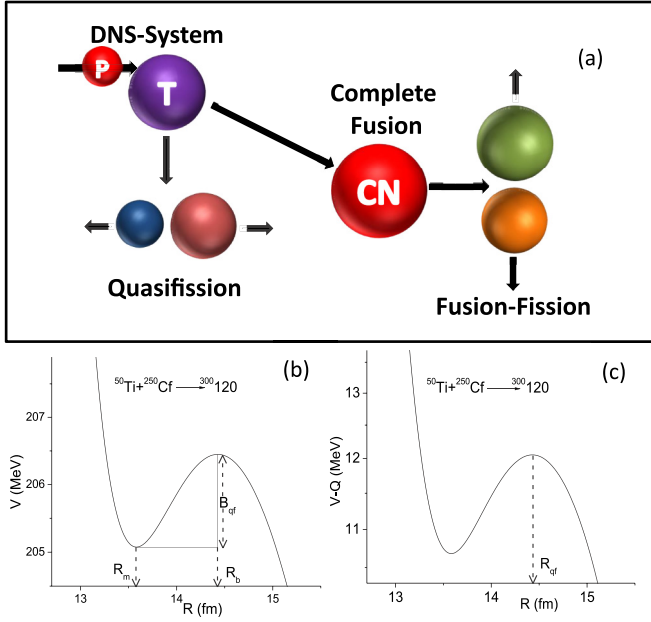
FIG. 1. (a) Schematic of the DNS model, (b) quasifission barrier, and (c) driving potential.

$$\times \exp\left(-\frac{B_{\mathrm{qf}}(Z, A, \ell)}{\Theta_{\mathrm{DNS}}(Z, A)}\right). \tag{2}$$

Here, the quantity Γ denotes an average width of the contributing single-particle states near the Fermi surface and normally, its value is taken as 2 MeV. If we consider the DNS behaves like a harmonic oscillator in the nucleus-nucleus interaction potential $V(R)$, R=distance between the two centers, such that $V(R) = 0$ at $R = R_m$. In this case, ω_m is the frequency of the harmonic oscillator and it is evaluated using the following equation:

$$\omega_m = \sqrt{\frac{A_1 + A_2}{A_1 A_2}\left(\frac{\partial^2 V(R)}{\partial R^2}\right)}\Bigg|_{R=R_m}. \tag{3}$$

Whereas ω_{qf} is the frequency of the inverted harmonic oscillator, while $V(R = R_B = R_{\mathrm{qf}}) = B_{\mathrm{fu}} = B_{\mathrm{qf}}$ (Fig. 1),

$$\omega_{\mathrm{qf}} = \sqrt{\frac{A_1 + A_2}{A_1 A_2}\left(\frac{\partial^2 V(R)}{\partial R^2}\right)}\Bigg|_{R=R_{\mathrm{qf}}}. \tag{4}$$

A_1 and A_2 are the mass numbers of quasifission fragments. The quasifission barrier $B_{\mathrm{qf}}(Z, A, \ell)$ in the dinuclear system as shown in Fig. 1 is expressed as

$$B_{\mathrm{qf}}(Z, A, l) = V(R_b, Z, A, \beta_{21}, \beta_{22}, l)$$
$$- V(R_m, Z, A, \beta_{21}, \beta_{22}, l), \tag{5}$$

where ℓ is the angular momentum. The nucleus-nucleus potential is minimum at distance $R = R_m$. For the pole-pole (tip-tip) orientation, it is expressed as

$$R_m = R_1\left[1 + \sqrt{\frac{5}{4\pi}}\beta_{21}\right] + R_2\left[1 + \sqrt{\frac{5}{4\pi}}\beta_{22}\right] + 0.5 \text{ fm}. \tag{6}$$

β_{21} and β_{22} are the quadruple deformation parameters of the nuclei forming the dinuclear system. R_1 and R_2 are the radii of the dinuclear system and it is evaluated using the expression as follows:

$$R_i = 1.23 A_i^{1/3} - \frac{0.98}{A_i^{1/3}}. \tag{7}$$

The position of the Coulomb barrier in the DNS is expressed as $R_b = R_{\mathrm{qf}} \approx R_m + 1.5$ fm. The local temperature of the dinuclear system over the quasifission barrier is given by

$$\Theta_{\mathrm{DNS}}(Z, A) = \sqrt{\left(\frac{E_{\mathrm{DNS}} - B_{\mathrm{qf}}}{a}\right)}. \tag{8}$$

The excitation energy of dinuclear system is expressed as

$$E_{\mathrm{DNS}} = E_{\mathrm{c.m.}} - V(R_m), \tag{9}$$

where $E_{\mathrm{c.m.}}$ is the center of mass energy. The level density parameters are given by $a = 0.134A - 1.21 \times 10^{-4}A^2$. The nucleus-nucleus interaction potential of the dinuclear system is given by [47]

$$V(R, Z_1, Z_2, \beta_{2i}, l) = V_c(R, Z_1, Z_2, \beta_{2i}) + V_N(R, Z_1, Z_2, \beta_{2i})$$
$$+ V_{\mathrm{rot}}(l, \beta_{2i}), \tag{10}$$

where V_C, V_N, and V_{rot} are the Coulomb, nuclear and rotational potentials, respectively. The Coulomb potential is given by

$$V_C(R, Z_1, Z_2, \beta_{2i}) = \frac{Z_1 Z_2}{R}e^2 + \frac{Z_1 Z_2}{R^3}e^2$$
$$\times\left[\left(\frac{9}{20\pi}\right)^{1/2}\sum_{i=1}^{2} R_i^2 \beta_{2i} P_2(\cos\alpha_i)\right.$$
$$\left. + \frac{3}{7\pi}\sum_{i=1}^{2} R_i^2[\beta_{2i} P_2(\cos\alpha_i)]^2\right]. \tag{11}$$

Z_1 and Z_2 are the charges of the nuclei forming the DNS. P_1 and P_2 are the Legendre polynomial of the nuclei forming the DNS expressed as

$$P_i(\cos\alpha_i) = \tfrac{1}{4}(1 + 3\cos 2\alpha_i). \tag{12}$$

α_i, $i = 1, 2$ is the orientation angle between the beam axis and symmetry axis of a deformed nucleus [49]. The nuclear potential is defined as

$$V_N(R, Z_1, Z_2, \beta_{2i}) = V_o\left\{\exp\left[\frac{-2(R - R_{12})\alpha}{R_{12}}\right]\right.$$
$$\left. - 2\exp\left[\frac{-(R - R_{12})\alpha}{R_{12}}\right]\right\}. \tag{13}$$

The strength of the potential V_o is given by

$$V_o = 2\pi a_1 a_2 \overline{R}(11.3 - 0.82\overline{R}_0)$$
$$\times\left(1 + \frac{0.16(\sum_{i=1}^{2} \beta_{2i})}{(1 + \exp[-17(|\eta| - 0.5)])}\right). \tag{14}$$

The surface diffuseness parameter of the heavy and light nuclei in the DNS are expressed as

$$a_1 = 0.56 \text{ fm} \quad \text{and} \quad a_2 = a_1 - 0.015|\eta|. \tag{15}$$

The mass asymmetry η is

$$\eta = \frac{A_1 - A_2}{A_1 + A_2}. \tag{16}$$

The quantity R_{12} is determined by

$$R_{12} = D_1 + D_2 + 0.1 \text{ fm}, \tag{17}$$

where

$$D_i(i = 1, 2) = R_i \left[1 + \left(\frac{5}{4\pi} \right)^{1/2} \beta_{2i} - \frac{1}{4\pi} \beta_{2i}^2 \right]. \tag{18}$$

The quantity α used in Eq. (13) is given by

$$\alpha = (11.47 - 17.32 a_1 a_2 + 2.07 \overline{R}_0)$$
$$\times \left[1 + 0.25 \sum_{i=1}^{2} \beta_{2i} \right]. \tag{19}$$

The quantities $\overline{R}_0$ and $\overline{R}$ used in Eq. (14) are defined as

$$\overline{R}_0 = \frac{R_1 R_2}{R_1 + R_2} \tag{20}$$

and

$$\overline{R} = \frac{\overline{R}_1 \overline{R}_2}{\overline{R}_1 + \overline{R}_2}. \tag{21}$$

The quantity $\overline{R}_i$ is given by

$$\overline{R}_i = D_i \frac{\left(1 + \left(\frac{5}{4\pi} \right)^{1/2} \beta_{2i} - \frac{1}{4\pi} \beta_{2i}^2 \right)}{1 + 4 \left(\frac{5}{5\pi} \right)^{1/2} \beta_{2i} - \frac{1}{4\pi} \beta_{2i}^2}. \tag{22}$$

The rotational potential of the DNS is defined as

$$V_{\text{rot}}(R, l, \beta_{2i}) = \frac{\hbar^2 \ell(\ell + 1)}{2 \text{Im}_{\text{DNS}}(R, A, \beta_{2i})}, \tag{23}$$

where ℓ is the angular momentum and Im_{DNS} is the moment of inertia of the DNS calculated as

$$\text{Im}_{\text{DNS}}(R, A, \beta_{2i}) = \text{Im}_1 + \text{Im}_2 + \mu R^2, \tag{24}$$

where $\text{Im}_i (i = 1, 2)$ is the moment of inertia of the DNS nuclei expressed as

$$\text{Im}_i = \tfrac{1}{5} m_0 A_i (a_i^2 + b_i^2), \tag{25}$$

where

$$a_i = R_i \left(1 - \frac{\beta_{2i}^2}{4\pi} \right) \left(1 + \sqrt{\frac{5}{4\pi}} \beta_{2i} \right), \tag{26}$$

$$b_i = R_i \left(1 - \frac{\beta_{2i}^2}{4\pi} \right) \left(1 + \sqrt{\frac{5}{16\pi}} \beta_{2i} \right), \tag{27}$$

and m_0 is the mass of a nucleon.

The driving potential is written as

$$U(Z, A, R) = V(R, Z_1, Z_2, \beta_{2i}, l) - Q \tag{28}$$

and the mass excess energy Q is as follows:

$$Q = B_1(Z_1) + B_2(Z_2) - B_{\text{CN}}(Z_{\text{CN}}), \tag{29}$$

where $B_1(Z_1)$, $B_2(Z_2)$, and $B_{\text{CN}}(Z_{\text{CN}})$ are the binding energies of the fragments in the DNS at their ground states and of the

compound nucleus, respectively, which are taken from [50]. Driving potential is shown in Fig. 1 as per the basis of the DNS model.

B. Fusion-fission lifetime

The fusion-fission lifetime of DNS is given by [48]

$$\tau_{\text{ff}} = \frac{1}{\lambda_{\text{ff}}}, \tag{30}$$

where λ_{ff} is the fusion-fission decay constant expressed as

$$\lambda_{\text{ff}} = \frac{1}{2\pi} \left(\sqrt{\left(\frac{\Gamma_0}{2\hbar} \right)^2 + \omega_f^2} - \frac{\Gamma_0}{2\hbar} \right)$$
$$\times \exp \left(-\frac{B_f(Z, A, \ell)}{\Theta(Z, A)} \right). \tag{31}$$

Here, ω_f is the frequency of the inverted oscillator that approximate the potential in the ground state and around the top of the fission barrier as

$$\omega_f = 0.5 \text{ MeV} \quad \text{and} \quad \Gamma_0 = 2 \text{ MeV}. \tag{32}$$

The fission barrier is given by the relation

$$B_f(\ell, \Theta) = c B_f^m(\ell) - h(\Theta) q(\ell) \partial W, \tag{33}$$

where $\text{B}_f^m(\ell)$ is the macroscopic part of fission barrier. This quantity depends on the angular momentum ℓ and it is parametrized by Sierk according to the rotating finite range model [51]. The microscopic part of the fission barrier including shell correction $\delta W = \delta W_{sad} - \delta W_{gs}$ is taken from Ref. [52]. The microscopic part of fission barrier consists of the damping of microscopic fission barrier on the excitation energy $h(\Theta)$ and angular momentum of a fissioning nucleus $q(\ell)$ is taken into account by the following relations [53]:

$$h(\Theta) = \left\{ 1 + \exp \left[\frac{(\Theta - \Theta_0)}{d} \right] \right\}^{-1} \tag{34}$$

and

$$q(l) = \left\{ 1 + \exp \left[\frac{(l - l_{1/2})}{\Delta l} \right] \right\}^{-1}. \tag{35}$$

The constants for the macroscopic fission barrier scaling, temperature, and angular momentum dependencies of the microscopic correction are chosen as $c = 1.0$, $d = 0.3$ MeV, $\ell_{1/2} = 20\hbar$ for nuclei with $Z = 80$–100, $\Delta \ell = 3\hbar$, and $\theta_0 = 1.16$ MeV [54]. The nuclear temperature depending on the level density parameter a is given by

$$\Theta(Z, A) = \sqrt{\frac{E_{\text{CN}}^*(l)}{a}}. \tag{36}$$

The excited energy of the compound nucleus is expressed as

$$E_{\text{CN}}^*(l) = E_{\text{c.m.}} + Q - V_{\text{rot}}^{CN}. \tag{37}$$
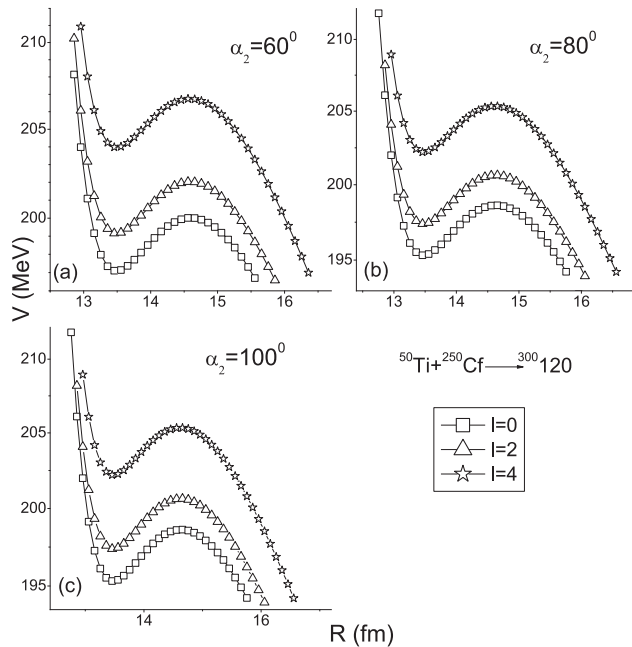
Q is defined in Eq. (29).

FIG. 2. The variation of nucleus-nucleus interaction potential of the dinuclear system with the mean distance between their centers for different angular momentum and different orientations of the target nuclei.

FIG. 3. The quasifission lifetime of the excited dinuclear system versus the center of mass energy $E_{c.m.}$ for different angular momentum ℓ and different orientation angles of the target nucleus α_2.

III. RESULTS AND DISCUSSION

We have studied the quasifission and fusion lifetimes for the projectile-target combinations such as ^{50}Ti $+ ^{246-252}$Cf, ^{54}Cr $+ ^{248}$Cm, ^{58}Fe $+ ^{244}$Pu, and ^{238}U $+ ^{60,64}$Ni as used for the synthesis of the superheavy element $Z = 120$. For an instance, the nucleus-nucleus interaction for the reaction ^{50}Ti $+ ^{250}$Cf $\rightarrow ^{300}$120 is shown in Fig. 1. The quasifission barrier is marked according to the definition given in Eq. (5). Here, the potential minimum appears at $R_m = 13.6$ fm and the quasifission barrier B_{qf} at $R_b = 14.4$ fm. The interaction potential at different target orientation such as $40°, 60°$, and $80°$ differ slightly as presented in Fig. 2. From this figure it is found that the interaction potential increases with an increase in the angular momentum, whereas the depth of the quasifission barrier B_{qf} decreases with the increase in the angular momentum. This implies that the quasifission probability increases with increase of the angular momentum. The depth of the quasifission barrier B_{qf} also increases with the increase in the orientation angle of the target nuclei. Thus, the contribution of the quasifission gets reduced to some extent by increasing the orientation angle of the target nuclei. To know the orientation angle, one may simulate the measured mass-angle distributions of the fragments from a reaction using a phenomenological model [55,56]. The maximum evaporation residue cross section is occurred at the optimal beam energy [57,58] when collision takes place on the equatorial sides of the target nucleus [57,59]. The reason of occurrence is well explained in Fazio *et al.* [57] in terms of dependence of Coulomb barrier on target orientation angle. The Coulomb barrier increases with the target orientation angle and reaches its maximum value at $90°$ (equatorial collision) while the
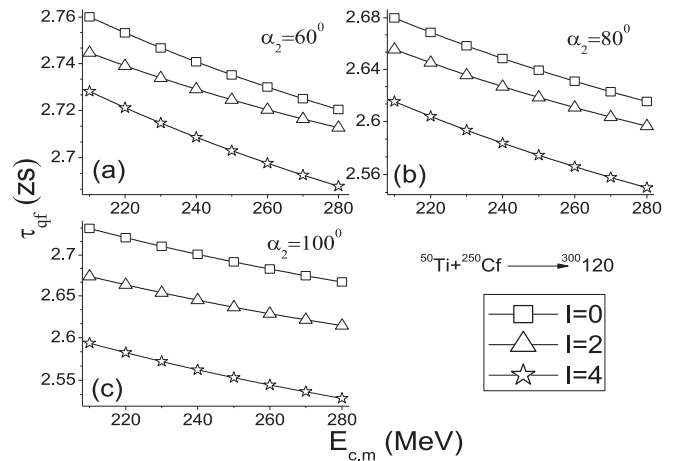
relative distance between the centres of the two interacting nuclei is minimum.

Figure 3 shows the behavior of the quasifission lifetime (τ_{qf}) of the excited dinuclear system versus the center of mass energy for different angular momentum at different orientations of the target nucleus. The quasifission lifetime decreases with the center of mass energy and angular momentum for a given orientation angle and increases with increasing orientation angle. Note that the said variation of τ_{qf} is too small to be differentiated in an experiment.

The variation of the fusion-fission decay constant [Fig. 4(a)] as well as fusion-fission lifetime [Fig. 4(b)] are shown with the center of mass energy for the projectile-target combination of ^{50}Ti $+ ^{249-252}$Cf, ^{54}Cr $+ ^{248}$Cm, ^{58}Fe $+ ^{244}$Pu, and ^{238}U $+ ^{60,64}$Ni. For these projectile-target combinations the fusion-fission decay constant increases with the center of mass energy. The variation of the fission barrier [Fig. 4(c)] and fusion-fission lifetime [Fig. 4(d)] are displayed with the angular momentum. This figure depicts that both the fission barrier and fusion-fission lifetime decrease with the increase of angular momentum. More specifically, the fusion-fission lifetime decreases with the increase of the angular momentum up to a certain ℓ value and then shows an appearance of constant value. However, such variations are too little to be realized in an experiment.

We have also plotted the quasifission lifetime of all possible projectile-target combinations such as ^{50}Ti $+ ^{249-252}$Cf, ^{54}Cr $+ ^{248}$Cm, ^{58}Fe $+ ^{244}$Pu, and ^{238}U $+ ^{60,64}$Ni with the fusion barrier and quasifission fission barrier in Fig. 5 and also the fusion-fission lifetime as a function of the fusion barrier and fission barrier of the compound superheavy nuclei. Even though excitation energy is kept constant to 50 MeV for every reaction, still no general trend is found in Fig. 5 for either the quasifission or fusion-fission lifetime. This reiterates the fact that these reactions involves a multiparametric puzzle, where deformation of colliding partners, incident energy, quasifission barrier, fusion barrier and excitation energy, binding energies for neutron and charged particles, fission barrier, binding energy of
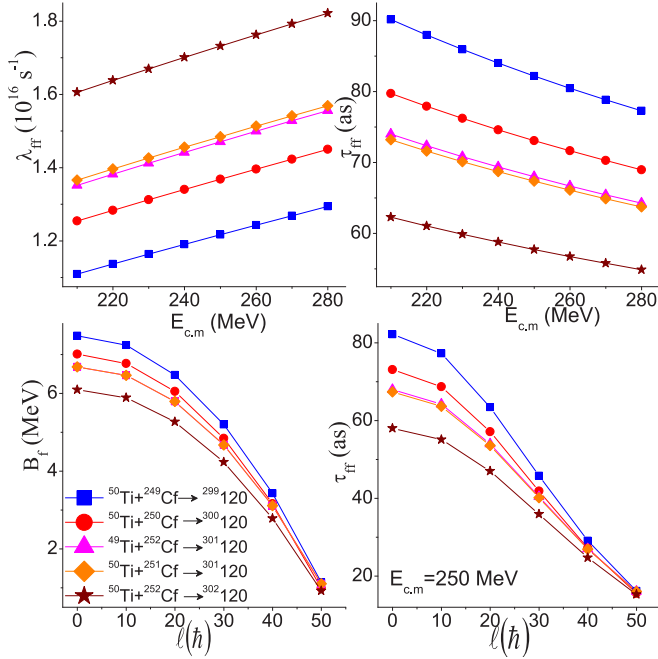
FIG. 4. The variation of the fusion-fission decay constant (a) and fusion-fission lifetime (b) with the center of mass energy $E_{c.m.}$. The fission barrier (c) and fusion-fission lifetime (d) as a function of the angular momentum ℓ.
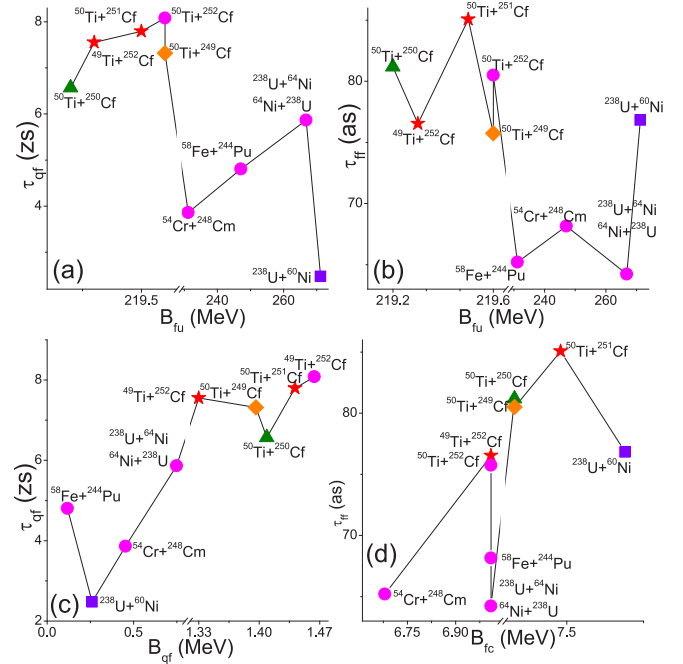

FIG. 5. The variation of the quasifission lifetime (a) and fusion-fission lifetime (b) with the fusion barrier B_{fu}. The quasifission lifetime vs the fission barrier of the heavier nucleus B_{fh} among the projectile and target nuclei (c). The fusion-fission lifetime vs the fission barrier of the compound nucleus B_{fc} formed (d).

intermediate excited nuclei in the de-excitation cascade of compound nucleus can play a determinant role. Whatsoever, the variation of the quasifission lifetime takes place with standard range of 2–9 zs and that of the fusion-fission lifetime is within 20 as.

Table I shows the fusion barrier, center of mass energy, laboratory energy, capture cross section, fusion cross section, evaporation cross section, evaporating neutron channel, fusion-fission cross section, quasifission lifetime, fusion-fission lifetime, and quasifission cross section for different

projectile-target combinations to synthesizing the superheavy element 120. Note that during the estimation of the evaporation residue cross section, we have considered average of the all possible orientation angles. Furthermore, we have not included the charged particle channels due to their small probabilities compared to the neutron channels. We have considered 1*n* to 6*n* channels in the calculation, but the evaporation residue cross sections of the most probable channels

TABLE I. Fusion barrier (B_{fu}), center of mass energy $E_{c.m.}$, laboratory energy E_{lab}, fusion cross section σ_{fus}, evaporation cross section σ_{er}, evaporating neutron channel (Ch.), fusion-fission cross section σ_{ff}, quasifission cross section σ_{qf}, quasifission lifetime τ_{qf}, and fusion-fission lifetime τ_{ff} for different projectile-target combinations, which were used to synthesize the superheavy element $Z = 120$. Note that the B_{fu} values are taken from Ref. [60]. Note that we have not included the charged particle channels due to their small probabilities compared to the neutron channels. We have considered 1*n* to 6*n* channels in the calculation, but the most probable channel is mentioned under the column title Ch.

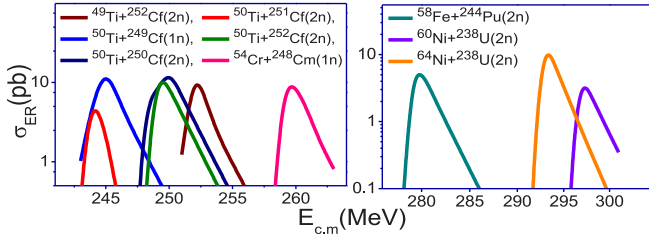| Reaction	B_{fu} MeV	$E_{c.m.}$ MeV	E_{lab} MeV	σ_{cap} mb	σ_{fus} mb	σ_{er} pb	Ch.	σ_{ff} mb	σ_{qf} mb	τ_{qf} zs	τ_{ff} as
$^{50}_{22}$Ti + $^{252}_{98}$Cf → ^{302}120	219.2	249	299	237.7	229.4	14.2	2	227.7	3.9	5.7	79.9
$^{50}_{22}$Ti + $^{251}_{98}$Cf → ^{301}120	219.3	244	293	288.5	276.6	16.3	1	275.9	6.4	7.1	75.3
$^{50}_{22}$Ti + $^{250}_{98}$Cf → ^{300}120	219.5	250	300	248.3	239.5	14.4	2	238.6	4.6	5.8	83.3
$^{49}_{22}$Ti + $^{252}_{98}$Cf → ^{301}120	219.6	250	299	245.7	237.8	15.9	2	234.9	5.2	5.5	74.1
$^{50}_{22}$Ti + $^{249}_{98}$Cf → ^{299}120	219.6	245	295	294.4	286.7	14.9	1	285.7	5.2	6.7	80.2
$^{54}_{24}$Cr + $^{248}_{96}$Cm → ^{302}120	231.2	259	316	280.4	271.9	9.9	1	270.4	4.6	3.9	64.8
$^{58}_{26}$Fe + $^{244}_{94}$Pu → ^{302}120	247.1	280	347	256.4	248.2	5.6	2	247.5	4.3	4.6	66.6
$^{64}_{28}$Ni + $^{238}_{92}$U → ^{302}120	266.8	293	372	260.4	248.8	3.1	2	246.9	8.3	4.3	63.3
$^{238}_{92}$U + $^{64}_{28}$Ni → ^{302}120	266.8	293	1383	260.4	248.8	3.1	2	246.9	8.3	4.3	63.3
$^{238}_{92}$U + $^{60}_{28}$Ni → ^{298}120	271.2	297	1476	279.6	272.6	4.2	2	271.4	3.7	2.7	74.1

FIG. 6. Excitation functions for the evaporation residue cross section for certain neutron channel mentioned alongside various nuclear reactions and as listed in Table I for synthesizing the superheavy nuclei $Z = 120$.

for every reaction is mentioned in the Table I as well as the excitation functions in Fig. 6. The reliability of these calculations can be realized by the fact that the relations $\sigma_{qf} = \sigma_{cap} - \sigma_{fus}$ and $\sigma_{er} = \sigma_{fus} - \sigma_{ff}$ are valid within 1% uncertainty. We can notice that the quasifission lifetime varies in the range of 3–7 zs and is in well accord with a recent work [61]. Though the values are quite close to the reaction contact times as measured in a recent experiment [62], but the contact times is no way related to the quasifission rather the deep inelastic time scales. According to Toke *et al.* [63], if full shape and energy relaxation takes place on the way from the contact configuration to the conditional saddle the system and is driven outwards in a deep inelastic process. On the other hand, if there is sufficient inward momentum to pass inside the conditional saddle, the system will be captured. It will gain sufficient time to experience a drift in mass asymmetry

towards lower or even vanishing saddle configurations. The result terminates to a quasifission process. This is why quasifission varies with the reactions from a few zs to tens of zs, whereas the contact times is nearly constant 2–3 zs [62].

The fusion-fission lifetime is nearly constant ≈ 13 as and the largest evaporation residue cross sections fall in the range of 3–16 pb (Table I). Hence, such data are quite conducive to experimentally observe the evaporation residues. However, practically, this scenario was not at all realized. This circumstances compel us to validate the present work through the experimentally known nuclear reactions. We have compared the theoretically calculated values in the framework of the present method with that of the available experimental values in Table II. From this comparison it is observed that the values produced by the present method are very close to the experiments. However, we do not get any clue why all the experimental attempts failed to observe the superheavy element $Z = 120$ mentioned in Table I.

In the next attempt, we have studied several successful and failed reactions used to synthesize various superheavy nuclei with respect to the fusion barrier (B_{fu}), Coulomb interaction parameter ($Z_1 Z_2$), mass asymmetry parameter η, fissility parameter (x_m), quasifission lifetime (τ_{qf}), fusion-fission lifetime (τ_{ff}), nuclear deformation parameters of the projectile and target, and fission barrier of the compound nucleus (B_{fc}) in Table III. Here, we notice a significant point as follows: the successful experiments included in either the projectile or target nucleus is spherical, or both the projectile and target nuclei are nearly spherical. This condition does not get satisfied for the first three failed reactions. However, though the next three

TABLE II. Comparison of the experimental (Ex.) and present theoretical (Th.) values of the quasifission lifetime τ_{qf} and fusion-fission lifetime τ_{ff}. The B_{fu} values are taken from Ref. [60].

Reaction	$E_{c.m.}$ (MeV)	B_{fu} (MeV)	τ_{ff} (as) Ex.	τ_{ff} (as) Th.	τ_{qf} (zs) Ex.	τ_{qf} (zs) Th.
$^{238}_{92}U + ^{65}_{30}Zn \rightarrow ^{303}122$ [63]	275.7	301.9	–	1.4	13.9	17.5
$^{238}_{92}U + ^{40}_{20}Ca \rightarrow ^{278}_{112}Cn$ [63]	184.9	196.0	–	1.4	13.9	11.9
$^{238}_{92}U + ^{48}_{20}Ca \rightarrow ^{278}_{112}Cn$ [63]	215.7	191.2	–	1.5	6.2	4.5
$^{238}_{92}U + ^{35}_{17}Cl \rightarrow ^{273}_{109}Mt$ [63]	204.4	166.5	–	1.6	9.1	8.9
$^{238}_{92}U + ^{16}_{32}S \rightarrow ^{108}_{270}Hs$ [63]	152.0	159.5	–	1.7	8.6	8.9
$^{32}_{72}Ge + ^{74}_{184}W \rightarrow ^{256}_{106}Sg$ [64]	178.1	245.4	1.6	1.8	–	5.4
$^{238}_{92}U + ^{13}_{27}Al \rightarrow ^{105}_{265}Db$ [63]	146.0	131.3	–	2.3	8.7	9.4
$^{28}_{64}Ni + ^{74}_{184}W \rightarrow ^{102}_{248}No$ [65]	341.0	217.7	1.0	1.5	5.0	2.4
$^{28}_{58}Ni + ^{74}_{184}W \rightarrow ^{102}_{242}No$ [64]	250.9	220.1	1.2	1.5	–	2.4
$^{28}_{58}Ni + ^{74}_{184}W \rightarrow ^{102}_{242}No$ [64]	266.1	220.1	1.4	1.5	–	2.3
$^{28}_{58}Ni + ^{74}_{184}W \rightarrow ^{102}_{242}No$ [64]	285.1	220.1	1.2	1.5	–	2.6
$^{22}_{48}Ti + ^{74}_{186}W \rightarrow ^{96}_{234}Cm$ [65]	245.0	176.1	1.3	2.4	10.0	9.8
$^{22}_{48}Ti + ^{74}_{184}W \rightarrow ^{96}_{232}Cm$ [64]	190.3	176.6	1.2	2.5	–	1.1
$^{22}_{48}Ti + ^{74}_{184}W \rightarrow ^{96}_{232}Cm$ [64]	194.3	176.6	1.0	2.5	–	1.1
$^{22}_{48}Ti + ^{74}_{184}W \rightarrow ^{96}_{232}Cm$ [64]	202.2	176.6	0.7	2.5	–	1.3
$^{8}_{16}O + ^{82}_{208}Pb \rightarrow ^{90}_{224}Th$ [66]	140.0	74.2	2.9	2.3	–	8.4
$^{16}_{32}S + ^{74}_{186}W \rightarrow ^{90}_{218}Th$ [65]	180.0	137.8	–	9.8	10.0	8.6
$^{16}_{32}S + ^{74}_{184}W \rightarrow ^{90}_{216}Th$ [64]	153.3	138.3	3.0	2.9	–	1.4

TABLE III. Comparison between the failed (F) and successful (S) experiments to synthesizing the superheavy nuclei with respect to the fusion barrier (B_{fu}), Coulomb interaction parameter (Z_1Z_2), mass asymmetry parameter η, fissility parameter (χ_m), quasifission lifetime (τ_{qf}), fusion-fission lifetime (τ_{ff}), nuclear deformation parameters of the projectile and target, and fission barrier of the compound nucleus (B_{fc}).

Reaction	B_{fu} [60] (MeV)	$B_{\mathrm{fu}}^{\mathrm{Bass}}$ (MeV)	Z_1Z_2	χ_m	η	$E_{\mathrm{c.m.}}$ (MeV)	E_{lab} (MeV)	τ_{qf} (zs)	τ_{ff} (as)	β_2 Proj.	β_2 Targ.	B_{fc} (MeV)	Rem.
$^{54}_{24}\mathrm{Cr} + ^{248}_{96}\mathrm{Cm} \rightarrow ^{302}120$ [9]	241.1	240.4	2304	0.87	−0.64	268	326	6.6	54.7	0.180	0.230	6.1	F
$^{58}_{26}\mathrm{Fe} + ^{244}_{94}\mathrm{Pu} \rightarrow ^{302}120$ [67]	255.5	254.2	2444	0.89	−0.62	263	325	4.6	54.1	0.199	0.224	6.1	F
$^{64}_{28}\mathrm{Ni} + ^{238}_{92}\mathrm{U} \rightarrow ^{302}120$ [68]	268.5	260.4	2576	0.91	−0.58	275	349	7.2	51.7	−0.087	0.215	6.1	F
$^{50}_{22}\mathrm{Ti} + ^{249}_{98}\mathrm{Cf} \rightarrow ^{299}120$ [69]	231.9	226.2	2208	0.85	−0.66	227	273	19.7	86.5	0	0.235	7.48	F
$^{50}_{22}\mathrm{Ti} + ^{249}_{97}\mathrm{Bk} \rightarrow ^{299}119$ [69]	223.9	223.7	2134	0.84	−0.66	222	267	25.1	94.5	0	0.235	7.72	F
$^{51}_{23}\mathrm{V} + ^{248}_{96}\mathrm{Cm} \rightarrow ^{299}119$ [70]	231.9	231.6	2208	0.86	−0.66	230	277	14.6	91.9	0	0.235	7.72	F
$^{48}_{20}\mathrm{Ca} + ^{249}_{98}\mathrm{Cf} \rightarrow ^{297}_{118}\mathrm{Og}$ [71]	205.4	205.5	1960	0.79	−0.68	197	235	340.6	130.1	0	0.235	8.49	S
$^{48}_{20}\mathrm{Ca} + ^{249}_{97}\mathrm{Bk} \rightarrow ^{297}_{117}\mathrm{Ts}$ [72]	203.2	203.2	1940	0.79	−0.68	200	239	190.3	154.7	0	0.235	9.1	S
$^{48}_{20}\mathrm{Ca} + ^{248}_{96}\mathrm{Cm} \rightarrow ^{296}_{116}\mathrm{Lv}$ [73]	201.1	201.1	1920	0.79	−0.67	202	241	145.5	155.1	0	0.235	9.1	S
$^{48}_{20}\mathrm{Ca} + ^{243}_{95}\mathrm{Am} \rightarrow ^{291}_{115}\mathrm{Mc}$ [74]	199.7	199.7	1900	0.79	−0.67	207	248	88.1	172.2	0	0.224	9.6	S
$^{48}_{20}\mathrm{Ca} + ^{242}_{94}\mathrm{Pu} \rightarrow ^{290}_{114}\mathrm{Fl}$ [73]	197.7	197.6	1880	0.78	−0.67	204	244	119.9	192.2	0	0.224	9.89	S
$^{70}_{30}\mathrm{Zn} + ^{209}_{83}\mathrm{Bi} \rightarrow ^{279}_{113}\mathrm{Nh}$ [75]	262.3	260.3	2490	0.88	−0.50	261	349	11.5	50.8	0.045	−0.008	6.12	S
$^{70}_{30}\mathrm{Zn} + ^{208}_{82}\mathrm{Pb} \rightarrow ^{278}_{112}\mathrm{Cn}$ [76]	259.0	257.2	2460	0.87	−0.50	259	346	6.5	49.5	0.045	0	5.99	S

reactions do satisfy the criterion, still the result is unfavorable. The only reason we can see is that the pb cross sections were predicted in Table I at energies about 25–33 MeV higher than the fusion barrier energies. In contrast, the failed experiments were conducted around or below the fusion barrier and a much lower cross section is evolved. A very recent work shows that the fusion probability drops down by a factor of 10^3 in the $^{54}\mathrm{Cr} + ^{248}\mathrm{Cm}$ reaction compared to the reactions of $^{48}\mathrm{Ca}$ ions with actinides at energies near the Coulomb barrier [61]. This aspect will be undertaken in a forthcoming work.

IV. CONCLUSIONS

The quasifission and fusion-fission lifetimes have been theoretically studied for the projectile-target combinations such as $^{50}\mathrm{Ti} + ^{249-252}\mathrm{Cf}$, $^{54}\mathrm{Cr} + ^{248}\mathrm{Cm}$, $^{58}\mathrm{Fe} + ^{244}\mathrm{Pu}$, and $^{238}\mathrm{U} + ^{60,64}\mathrm{Ni}$ which were used to synthesize the superheavy nuclei $Z = 120$. The effect of target orientation and angular momentum on the quasifission and fusion-fission lifetimes have been, in particular, emphasized. The theoretical methodology was well validated by the comparison

of the calculated values with the experimental data. Hence, the present work may be useful in the prediction of the quasifission and fusion-fission lifetimes for any superheavy nuclei.

Though above theoretical lifetime predictions are quite important, but this lifetime study does not spot any valid reason behind the failure of the attempted reactions to synthesizing the superheavy nuclei $Z = 120$. In next attempt, consideration of the fusion barrier, Coulomb interaction, fissility, mass asymmetry, deformation parameter, fission barrier, etc., leads us to reveal that either the projectile or target nucleus of a successful reaction was spherical. However, this condition alone does not ensure the synthesizing of the superheavy elements $Z > 118$. The final step is to choose the colliding energy so judiciously that the evaporation residue cross section with the chosen reaction is the largest and well within the experimental limitations. This scenario can be be seen ine Table I that the estimated σ_{er} are in the pb range at the optimal beam energies. To have confidence on these results, we have calculated the σ_{er} at the beam energies at which the experiments were preformed and reported in Table IV.

TABLE IV. DNS prediction of the evaporation residue cross section σ_{er} at the experimental condition for the reactions attempted for synthesizing the SHE $Z = 120$.

System	E^*	V_B	$E_{\mathrm{c.m.}}^{\mathrm{exp}}$	σ_{ER} (fb) 1n	2n	3n
$^{50}\mathrm{Ti} + ^{249}Cf \rightarrow ^{299}120$ [77]	31.7	219.6	226.7	–	1	0.2
$^{64}\mathrm{Ni} + ^{238}U \rightarrow ^{302}120$ [77]	27.3	266.9	264.7	–	–	10.6
$^{54}\mathrm{Cr} + ^{248}\mathrm{Cm} \rightarrow ^{302}120$ [77]	33.0	231.3	240.2	–	–	3.7
$^{58}\mathrm{Fe} + ^{244}\mathrm{Pu} \rightarrow ^{302}120$ [77]	33.9	247.0	253.9	–	–	1.6

It shows that the σ_{er} are all in fb and thereby, it has not been possible to have them measured. Hence, the present work may be of good help in taking the corrective measures for the forthcoming experimental attempts for the synthesis of the superheavy nuclei $Z = 120$.

[1] H. Haba, A new period in superheavy-element hunting, Nat. Chem. **11**, 10 (2019).

[2] S. Hofmann and G. Münzenberg, The discovery of the heaviest elements, Rev. Mod. Phys. **72**, 733 (2000).

[3] Y. Oganessian, Heaviest nuclei from 48ca-induced reactions, J. Phys. G: Nucl. Part. Phys. **34**, R165 (2007).

[4] Y. T. Oganessian and V. Utyonkov, Super-heavy element research, Rep. Prog. Phys. **78**, 036301 (2015).

[5] M. S. Lee, Elemental haiku, Science **357**, 461 (2017).

[6] G. Fazio, G. Giardina, A. Lamberto, R. Ruggeri, C. Saccá, R. Palamara, A. Muminov, A. Nasirov, U. Yakhshiev, F. Hanappe *et al.*, Formation of heavy and superheavy elements by reactions with massive nuclei, Eur. Phys. J. A **19**, 89 (2004).

[7] M. Itkis, E. Vardaci, I. Itkis, G. Knyazheva, and E. Kozulin, Fusion and fission of heavy and superheavy nuclei (experiment), Nucl. Phys. A **944**, 204 (2015).

[8] E. Vardaci, M. G. Itkis, I. M. Itkis, G. Knyazheva, and E. Kozulin, Fission and quasifission toward the superheavy mass region, J. Phys. G: Nucl. Part. Phys. **46**, 103002 (2019).

[9] S. Hofmann, S. Heinz, R. Mann, J. Maurer, G. Münzenberg, S. Antalic, W. Barth, H. Burkhard, L. Dahl, K. Eberhardt *et al.*, Review of even element super-heavy nuclei and search for element 120, Eur. Phys. J. A **52**, 180 (2016).

[10] S. A. Giuliani, Z. Matheson, W. Nazarewicz, E. Olsen, P.-G. Reinhard, J. Sadhukhan, B. Schuetrumpf, N. Schunck, and P. Schwerdtfeger, Colloquium: Superheavy elements: Oganesson and beyond, Rev. Mod. Phys. **91**, 011001 (2019).

[11] K. Novikov, E. Kozulin, G. Knyazheva, I. Itkis, A. Karpov, M. Itkis, I. Diatlov, M. Cheralu, B. Gall, Z. Asfari *et al.*, Formation and decay of the composite system $z = 120$ in reactions with heavy ions at energies near the Coulomb barrier, Bull. Russ. Acad. Sci.: Phys. **84**, 495 (2020).

[12] D. J. Hinde, Fusion and quasifission in superheavy element synthesis, Nucl. Phys. News **28**, 13 (2018).

[13] N. Antonenko, E. Cherepanov, A. Nasirov, V. Permjakov, and V. Volkov, Competition between complete fusion and quasifission in reactions between massive nuclei. The fusion barrier, Phys. Lett. B **319**, 425 (1993).

[14] N. V. Antonenko, E. A. Cherepanov, A. K. Nasirov, V. P. Permjakov, and V. V. Volkov, Compound nucleus formation in reactions between massive nuclei: Fusion barrier, Phys. Rev. C **51**, 2635 (1995).

[15] N. Antonenko, G. Adamian, W. Scheid, and V. Volkov, Competition between complete fusion and quasi-fission in dinuclear system, Il Nuovo Cimento A **110**, 1143 (1997).

[16] G. Adamian, N. Antonenko, and W. Scheid, Model of competition between fusion and quasifission in reactions with heavy nuclei, Nucl. Phys. A **618**, 176 (1997).

[17] N. Wang, J.-q. Li, and E.-g. Zhao, Orientation effects of deformed nuclei on the production of superheavy elements, Phys. Rev. C **78**, 054607 (2008).

[18] A. Diaz-Torres, G. G. Adamian, N. V. Antonenko, and W. Scheid, Quasifission process in a transport model for a dinuclear system, Phys. Rev. C **64**, 024604 (2001).

[19] G. G. Adamian, N. V. Antonenko, and W. Scheid, Characteristics of quasifission products within the dinuclear system model, Phys. Rev. C **68**, 034601 (2003).

[20] K. Godbey and A. S. Umar, Quasifission dynamics in microscopic theories, Front. Phys. **8**, 40 (2020).

[21] D. J. Hinde, R. du Rietz, M. Dasgupta, R. G. Thomas, and L. R. Gasques, Two distinct quasifission modes in the ^{32}S + ^{232}Th reaction, Phys. Rev. Lett. **101**, 092701 (2008).

[22] D. J. Hinde, M. Dasgupta, D. Y. Jeung, G. Mohanto, E. Prasad, C. Simenel, E. Williams, I. P. Carter, K. J. Cook, S. Kalkal *et al.*, Quasifission dynamics in the formation of superheavy elements, in *EPJ Web of Conferences* (EDP Sciences, Hobart, Tasmania, Australia, 2017), Vol. 163, p. 00023.

[23] B. B. Back, P. B. Fernandez, B. G. Glagola, D. Henderson, S. Kaufman, J. G. Keller, S. J. Sanders, F. Videbæk, T. F. Wang, and B. D. Wilkins, Entrance-channel effects in quasifission reactions, Phys. Rev. C **53**, 1734 (1996).

[24] K. Sekizawa and K. Hagino, Time-dependent Hartree-Fock plus Langevin approach for hot fusion reactions to synthesize the $z = 120$ superheavy element, Phys. Rev. C **99**, 051602(R) (2019).

[25] C. Schmitt, K. Mazurek, and P. N. Nadtochy, New procedure to determine the mass-angle correlation of quasifission, Phys. Rev. C **100**, 064606 (2019).

[26] K. Godbey, A. S. Umar, and C. Simenel, Deformed shell effects in ^{48}Ca + ^{249}Bk quasifission fragments, Phys. Rev. C **100**, 024610 (2019).

[27] C. Eccles, S. Roy, T. H. Gray, and A. Zaccone, Temperature dependence of nuclear fission time in heavy-ion fusion-fission reactions, Phys. Rev. C **96**, 054611 (2017).

[28] S. Q. Guo, Y. Gao, J. Q. Li, and H. F. Zhang, Dynamical deformation in heavy ion reactions and the characteristics of quasifission products, Phys. Rev. C **96**, 044622 (2017).

[29] V. E. Oberacker, A. S. Umar, and C. Simenel, Dissipative dynamics in quasifission, Phys. Rev. C **90**, 054605 (2014).

[30] E. Williams, D. J. Hinde, M. Dasgupta, R. du Rietz, I. P. Carter, M. Evers, D. H. Luong, S. D. McNeil, D. C. Rafferty, K. Ramachandran *et al.*, Evolution of signatures of quasifission in reactions forming curium, Phys. Rev. C **88**, 034611 (2013).

[31] V. L. Litnevsky, V. V. Pashkevich, G. I. Kosenko, and F. A. Ivanyuk, Influence of the shell structure of colliding nuclei in fusion-fission reactions, Phys. Rev. C **85**, 034602 (2012).

[32] C. Wong, Interaction Barrier in Charged-Particle Nuclear Reactions, Phys. Rev. Lett. **31**, 766 (1973).

[33] D. Jain, R. Kumar, M. K. Sharma, and R. K. Gupta, Skyrme forces and the fusion-fission dynamics of the ^{132}Sn + ^{64}Ni → ^{196}Pt reaction, Phys. Rev. C **85**, 024615 (2012).

[34] S. A. Kalandarov, G. G. Adamian, N. V. Antonenko, and W. Scheid, Role of angular momentum in the production of com-

plex fragments in fusion and quasifission reactions, Phys. Rev. C **83**, 054611 (2011).

[35] E. Prasad, K. M. Varier, R. G. Thomas, P. Sugathan, A. Jhingan, N. Madhavan, B. R. S. Babu, R. Sandal, S. Kalkal, S. Appannababu, J. Gehlot, K. S. Golda, S. Nath, A. M. Vinodkumar, B. P. AjithKumar, B. V. John, G. Mohanto, M. M. Musthafa, R. Singh, A. K. Sinha, and S. Kailas, Conclusive evidence of quasifission in reactions forming the ^{210}Rn compound nucleus, Phys. Rev. C **81**, 054608 (2010).

[36] K. Nishio, H. Ikezoe, I. Nishinaka, S. Mitsuoka, K. Hirose, T. Ohtsuki, Y. Watanabe, Y. Aritomo, and S. Hofmann, Evidence for quasifission in the sub-barrier reaction of ^{30}Si $+\,^{238}$U, Phys. Rev. C **82**, 044604 (2010).

[37] N. Wang, K. Zhao, W. Scheid, and X. Wu, Fusion-fission reactions with a modified Woods-Saxon potential, Phys. Rev. C **77**, 014603 (2008).

[38] J. Velkovska, C. R. Morton, R. L. McGrath, P. Chung, and I. Diószegi, Quasifission reactions as a probe of nuclear viscosity, Phys. Rev. C **59**, 1506 (1999).

[39] D. J. Hinde, M. Dasgupta, J. R. Leigh, J. C. Mein, C. R. Morton, J. O. Newton, and H. Timmers, Conclusive evidence for the influence of nuclear orientation on quasifission, Phys. Rev. C **53**, 1290 (1996).

[40] B. B. Back, S. Bjørnholm, T. Døssing, W. Q. Shen, K. D. Hildenbrand, A. Gobbi, and S. P. Sørensen, Relaxation of angular momentum in fission and quasifission reactions, Phys. Rev. C **41**, 1495 (1990).

[41] D. J. Hinde, H. Ogata, M. Tanaka, T. Shimoda, N. Takahashi, A. Shinohara, S. Wakamatsu, K. Katori, and H. Okamura, Systematics of fusion-fission time scales, Phys. Rev. C **39**, 2268 (1989).

[42] W. Q. Shen, J. Albinski, A. Gobbi, S. Gralla, K. D. Hildenbrand, N. Herrmann, J. Kuzminski, W. F. J. Müller, H. Stelzer, J. Tke, B. B. Back, S. Bjornholm, and S. P. Sorensen, Fission and quasifission in U-induced reactions, Phys. Rev. C **36**, 115 (1987).

[43] B. B. Back, Complete fusion and quasifission in reactions between heavy ions, Phys. Rev. C **31**, 2104 (1985).

[44] B. Tamain, F. Plasil, C. Ngô, J. Péter, M. Berlanger, and F. Hanappe, Energy Dependence of Quasifission, Phys. Rev. Lett. **36**, 18 (1976).

[45] P. Wen, C. Li, L. Zhu, C. Lin, and F. Zhang, Mechanism of multinucleon transfer reaction based on the grazing model and DNS model, J. Phys. G: Nucl. Part. Phys. **44**, 115101 (2017).

[46] P. Wen, A. Nasirov, C. Lin, and H. Jia, Multinucleon transfer reaction from view point of dynamical dinuclear system method, J. Phys. G: Nucl. Part. Phys. **47**, 075106 (2020).

[47] S. Soheyli and M. V. Khanlari, Theoretical study of effects of the entrance channel on the relative yield of complete fusion and quasifission in heavy-ion collisions within a dinuclear system approach, Phys. Rev. C **94**, 034615 (2016).

[48] M. V. Khanlari and S. Soheyli, Quasifission and fission rates and their lifetimes in asymmetric reactions forming ^{216}Ra within a dinuclear system approach, Phys. Rev. C **95**, 024617 (2017).

[49] A. Nasirov, A. Fukushima, Y. Toyoshima, Y. Aritomo, A. Muminov, S. Kalandarov, and R. Utamuratov, The role of orientation of nucleus symmetry axis in fusion dynamics, Nucl. Phys. A **759**, 342 (2005).

[50] G. Audi, A. Wapstra, and C. Thibault, The AME2003 atomic mass evaluation: (ii) Tables, graphs and references, Nucl. Phys. A **729**, 337 (2003).

[51] A. J. Sierk, Macroscopic model of rotating nuclei, Phys. Rev. C **33**, 2039 (1986).

[52] W. M. P. Moller, J.R. Nix, and W. Swiatecki, Nuclear ground-state masses and and deformations, At. Data Nucl. Data Tables **59**, 185 (1995).

[53] G. Mandaglio, G. Giardina, A. K. Nasirov, and A. Sobiczewski, Investigation of the ^{48}Ca $+\,^{249-252}$Cf reactions synthesizing isotopes of the superheavy element 118, Phys. Rev. C **86**, 064607 (2012).

[54] A. Nasirov, K. Kim, G. Mandaglio, G. Giardina, A. Muminov, and Y. Kim, Main restrictions in the synthesis of new superheavy elements: Quasifission and/or fusion fission, Eur. Phys. J. A **49**, 147 (2013).

[55] E. Prasad, A. Wakhle, D. J. Hinde, E. Williams, M. Dasgupta, M. Evers, D. H. Luong, G. Mohanto, C. Simenel, and K. Vo-Phuoc, Exploring quasifission characteristics for ^{34}S $+\,^{232}$Th forming ^{266}Sg, Phys. Rev. C **93**, 024607 (2016).

[56] E. Prasad, D. J. Hinde, E. Williams, M. Dasgupta, I. P. Carter, K. J. Cook, D. Y. Jeung, D. H. Luong, C. S. Palshetkar, D. C. Rafferty, K. Ramachandran, C. Simenel, and A. Wakhle, Fusion and quasifission studies for the ^{40}Ca $+\,^{186}$W, ^{192}Os reactions, Phys. Rev. C **96**, 034608 (2017).

[57] G. Fazio, G. Giardina, F. Hanappe, G. Mandaglio, M. Manganaro, A. I. Muminov, A. K. Nasirov, and C. Saccá, Role of the target orientation angle and orbital angular momentum in the evaporation residue production, J. Phys. Soc. Jpn. **77**, 124201 (2008).

[58] A. S. Umar, V. E. Oberacker, and C. Simenel, Fusion and quasifission dynamics in the reactions ^{48}Ca $+\,^{249}$Bk and ^{50}Ti $+\,^{249}$Bk using a time-dependent Hartree-Fock approach, Phys. Rev. C **94**, 024605 (2016).

[59] K. Nishio, H. Ikezoe, S. Mitsuoka, I. Nishinaka, Y. Nagame, Y. Watanabe, T. Ohtsuki, K. Hirose, and S. Hofmann, Effects of nuclear orientation on the mass distribution of fission fragments in the reaction of S 36+ U 238, Phys. Rev. C **77**, 064607 (2008).

[60] T. Nandi, D. K. Swami, P. S. Damodara Gupta, Y. Kumar, S. Chakraborty, and H. C. Manjunatha, Search for a good nucleus-nucleus potential applicable up to the reactions synthesizing the superheavy nuclei, private communication (2020).

[61] K. V. Novikov, E. M. Kozulin, G. N. Knyazheva, I. M. Itkis, M. G. Itkis, A. A. Bogachev, I. N. Diatlov, M. Cheralu, D. Kumar, N. I. Kozulina, A. N. Pan, I. V. Pchelintsev, I. V. Vorobiev, W. H. Trzaska, S. Heinz, H. M. Devaraja, B. Lommel, E. Vardaci, S. Spinosa, A. DiNitto, A. Pulcini, S. V. Khlebnikov, P. P. Singh, R. N. Sahoo, B. Gall, Z. Asfari, C. Borcea, I. Harca, and D. M. Filipescu, Investigation of fusion probabilities in the reactions with Cr 52, 54, Ni 64, and Zn 68 ions leading to the formation of $z = 120$ superheavy composite systems, Phys. Rev. C **102**, 044605 (2020).

[62] H. Albers, J. Khuyagbaatar, D. Hinde, I. Carter, K. Cook, M. Dasgupta, C. E. Düllmann, K. Eberhardt, D. Jeung, S. Kalkal *et al.*, Zeptosecond contact times for element $z = 120$ synthesis, Phys. Lett. B **808**, 135626 (2020).

[63] J. Tōke, R. Bock, G. Dai, A. Gobbi, S. Gralla, K. Hildenbrand, J. Kuzminski, W. Müller, A. Olmi, H. Stelzer *et al.*, Quasi-fission–the mass-drift mode in heavy-ion reactions, Nucl. Phys. A **440**, 327 (1985).

[64] J. U. Andersen, J. Chevallier, J. S. Forster, S. A. Karamian, C. R. Vane, J. R. Beene, A. Galindo-Uribarri, J. G. delCampo, C. J. Gross, H. F. Krause, E. Padilla-Rodal, D. Radford, D.

Shapira, C. Broude, F. Malaguti, and A. Uguzzoni, Attosecond time delays in heavy-ion induced fission measured by crystal blocking, Phys. Rev. C **78**, 064609 (2008).

[65] R. du Rietz, D. J. Hinde, M. Dasgupta, R. G. Thomas, L. R. Gasques, M. Evers, N. Lobanov, and A. Wakhle, Predominant time scales in fission processes in reactions of S, Ti and Ni with W: Zeptosecond versus attosecond, Phys. Rev. Lett. **106**, 052701 (2011).

[66] R. Butsch, D. J. Hofman, C. P. Montoya, P. Paul, and M. Thoennessen, Time scales for fusion-fission and quasifission from giant dipole resonance decay, Phys. Rev. C **44**, 1515 (1991).

[67] O. Y. Ts *et al.*, Attempt to produce element 120 in the ^{244}Pu + ^{58}Fe reaction II, Phys. Rev. C **79**, 024603 (2009).

[68] S. Hofmann, D. Ackermann, S. Antalic, V. F. Comas, S. Heinz *et al.*, Probing shell effects at $z = 120$ and $n = 184$, GSI Scientific Report No. 2008 (2009), p. 131.

[69] C. E. Düllmann, On the search for elements beyond $z = 118$. An outlook based on lessons from the heaviest known elements, in *EPJ Web of Conferences* (EDP Sciences, Stará Lesná, Slovakia, 2015), Vol. 131, p. 08004.

[70] K. Chapman, Hunt for element 119 set to begin, Chemistry World, 12th September 2017.

[71] Y. T. Oganessian, F. S. Abdullin, C. Alexander, J. Binder, R. A. Boll, S. N. Dmitriev, J. Ezold, K. Felker, J. M. Gostic, R. K. Grzywacz, J. H. Hamilton, R. A. Henderson, M. G. Itkis, K. Miernik, D. Miller, K. J. Moody, A. N. Polyakov, A. V. Ramayya, J. B. Roberto, M. A. Ryabinin, K. P. Rykaczewski, R. N. Sagaidak, D. A. Shaughnessy, I. V. Shirokovsky, M. V. Shumeiko, M. A. Stoyer, N. J. Stoyer, V. G. Subbotin, A. M. Sukhov, Y. S. Tsyganov, V. K. Utyonkov, A. A. Voinov, and G. K. Vostokin, Production and Decay of the Heaviest Nuclei $^{293-294}$117 and ^{294}118, Phys. Rev. Lett. **109**, 162501 (2012).

[72] Y. T. Oganessian, F. S. Abdullin, P. D. Bailey, D. E. Benker, M. E. Bennett, S. N. Dmitriev, J. G. Ezold, J. H. Hamilton, R. A. Henderson, M. G. Itkis, Y. V. Lobanov, A. N. Mezentsev, K. J. Moody, S. L. Nelson, A. N. Polyakov, C. E. Porter, A. V. Ramayya, F. D. Riley, J. B. Roberto, M. A. Ryabinin, K. P. Rykaczewski, R. N. Sagaidak, D. A. Shaughnessy, I. V.

Shirokovsky, M. A. Stoyer, V. G. Subbotin, R. Sudowe, A. M. Sukhov, Y. S. Tsyganov, V. K. Utyonkov, A. A. Voinov, G. K. Vostokin, and P. A. Wilk, Synthesis of a New Element with Atomic Number $z = 117$, Phys. Rev. Lett. **104**, 142502 (2010).

[73] Y. T. Oganessian, V. K. Utyonkov, Y. V. Lobanov, F. S. Abdullin, A. N. Polyakov, I. V. Shirokovsky, Y. S. Tsyganov, G. G. Gulbekian, S. L. Bogomolov, B. N. Gikal, A. N. Mezentsev, S. Iliev, V. G. Subbotin, A. M. Sukhov, A. A. Voinov, G. V. Buklanov, K. Subotic, V. I. Zagrebaev, M. G. Itkis, J. B. Patin, K. J. Moody, J. F. Wild, M. A. Stoyer, N. J. Stoyer, D. A. Shaughnessy, J. M. Kenneally, P. A. Wilk, R. W. Lougheed, R. I. Ilkaev, and S. P. Vesnovskii, Measurements of cross sections and decay properties of the isotopes of elements 112, 114, and 116 produced in the fusion reactions ^{233,238}U, ^{242}Pu, and ^{248}Cm + ^{48}Ca, Phys. Rev. C **70**, 064609 (2004).

[74] Y. T. Oganessian, V. K. Utyonkov, Y. V. Lobanov, F. S. Abdullin, A. N. Polyakov, I. V. Shirokovsky, Y. S. Tsyganov, G. G. Gulbekian, S. L. Bogomolov, A. N. Mezentsev, S. Iliev, V. G. Subbotin, A. M. Sukhov, A. A. Voinov, G. V. Buklanov, K. Subotic, V. I. Zagrebaev, M. G. Itkis, J. B. Patin, K. J. Moody, J. F. Wild, M. A. Stoyer, N. J. Stoyer, D. A. Shaughnessy, J. M. Kenneally, and R. W. Lougheed, Experiments on the synthesis of element 115 in the reaction ^{243}Am(^{48}Ca, xn)$^{291-x}$115, Phys. Rev. C **69**, 021601(R) (2004).

[75] K. Morita, K. Morimoto, D. Kaji, T. Akiyama, S.-i. Goto, H. Haba, E. Ideguchi, R. Kanungo, K. Katori, H. Koura *et al.*, Experiment on the synthesis of element 113 in the reaction ^{209}Bi (^{70}Zn, n) ^{278}113, J. Phys. Soc. Jpn. **73**, 2593 (2004).

[76] S. Hofmann, F. Heßberger, D. Ackermann, G. Münzenberg, S. Antalic, P. Cagarda, B. Kindler, J. Kojouharova, M. Leino, B. Lommel *et al.*, New results on elements 111 and 112, Eur. Phys. J. A **14**, 147 (2002).

[77] J. Khuyagbaatar, A. Yakushev, C. E. Düllmann, H. Nitsche, J. Roberto, D. Ackermann, L.-L. Andersson, M. Asai, H. Brand, M. Block *et al.*, The superheavy element search campaigns at Tasca, 2013.